Published in final edited form as:
*Nature*. 2014 May 22; 509(7501): 507–511. doi:10.1038/nature13324.

# MSFD2A is critical for the formation and function of the blood brain barrier

**Ayal Ben-Zvi**[1], **Baptiste Lacoste**[1], **Esther Kur**[1], **Benjamin J. Andreone**[1], **Yoav Mayshar**[2], **Han Yan**[1], and **Chenghua Gu**[1,3]

[1]Department of Neurobiology, Harvard Medical School, 220 Longwood Ave, Boston, MA 02115, U.S.A.

[2]Department of Genetics, Harvard Medical School, 220 Longwood Ave, Boston, MA 02115, U.S.A.

## Abstract

The central nervous system (CNS) requires a tightly controlled environment free of toxins and pathogens to provide the proper chemical composition for neural function. This environment is maintained by the 'blood brain barrier' (BBB), which is composed of blood vessels whose endothelial cells display specialized tight junctions and extremely low rates of transcellular vesicular transport (transcytosis)[1–3]. In concert with pericytes and astrocytes, this unique brain endothelial physiological barrier seals the CNS and controls substance influx and efflux[4–6]. While BBB breakdown has recently been associated with initiation and perpetuation of various neurological disorders, an intact BBB is a major obstacle for drug delivery to the CNS[7–10]. A limited understanding of the molecular mechanisms that control BBB formation has hindered our ability to manipulate the BBB in disease and therapy. Here, we identify mechanisms governing the establishment of a functional BBB. First, using a novel embryonic tracer injection method, we demonstrate spatiotemporal developmental profiles of BBB functionality and find that the mouse BBB becomes functional at embryonic day 15.5 (E15.5). We then screen for BBB-specific genes expressed during BBB formation, and find that *major facilitator super family domain containing 2a* (*Mfsd2a*) is selectively expressed in BBB-containing blood vessels in the CNS. Genetic ablation of *Mfsd2a* results in a leaky BBB from embryonic periods through adulthood, while maintaining the normal patterning of vascular networks. Electron microscopy examination reveals a dramatic increase in CNS endothelial cell vesicular transcytosis in *Mfsd2a*$^{-/-}$ mice, without obvious tight junction defects. Finally we show that MFSD2A endothelial expression is regulated by pericytes to facilitate BBB integrity. These findings identify MFSD2A as a key regulator of BBB function that may act by suppressing transcytosis in CNS endothelial cells. Further our findings may aid in efforts to develop therapeutic approaches for CNS drug delivery.

[3]Correspondence and requests for materials should be addressed to C.G. Chenghua Gu (chenghua_gu@hms.harvard.edu), Department of Neurobiology, Harvard Medical School Boston, MA 02115, U.S.A. (Ph) 617-432-6364 (Fax) 617-432-1639.

**Author Contributions**

C.G and A.B.Z conceived and designed the project.
A.B.Z, B.L, E.K, B.J.A, H.Y performed experiments.
A.B.Z and B.L analyzed data and preformed image analysis/quantification.
Y.M analyzed microarray data.
C.G and A.B.Z wrote the manuscript with significant input from B.L and B.J.A.

Two unique features of the CNS endothelium determine BBB integrity (Extended Data Fig. 1)[2]. One is specialized tight junctions between a single endothelial cell layer lining the CNS capillaries, which form the physical seal between the blood and brain parenchyma[2]. In addition, CNS endothelial cells have lower rates of transcytosis than endothelial cells in other organs[3]. Peripheral endothelial cells display active vesicle trafficking to deliver nutrients to peripheral tissues, while CNS endothelial cells express transporters to selectively traffic nutrients across the BBB[1, 3, 11]. However, it is not clear when and how these properties are acquired. Further, the molecular mechanisms that give rise to the unique properties of the CNS endothelium have not been identified. Although recent studies revealed molecular pathways involved in the development of the embryonic BBB[12–19], disruption of some of these genes affect vascular network development, making it difficult to determine whether barrier defects are primary or secondary to a broader vascular effect.

We aimed to first identify the developmental time-point when the BBB gains functional integrity, and then use that time window to profile BBB-specific genes when BBB is actively forming to maximize the chance of identifying key regulators. The prevailing view has been that the embryonic and perinatal BBB are not yet functional[1]. However, previous embryonic BBB functionality studies were primarily performed by trans-cardiac dye/tracer perfusion, which may dramatically affect blood pressure, cause bursting of CNS capillaries, and artificially produce leakiness phenotypes[1, 20]. To circumvent these obstacles, we developed a method to assess BBB integrity during mouse development, in which a small volume of tracer is injected into embryonic liver to minimize changes in blood pressure (Fig. 1a, supplementary information for method).

Using this method, we identified the timing of BBB formation in the developing mouse brain and observed a spatial and temporal pattern of functional barrier-genesis (Fig. 1b). We found that in E13.5 cortex a 10-kDa dextran tracer leaked out of capillaries and was taken up by non-vascular brain parenchyma cells (Fig. 1b, upper panel). At E14.5, the tracer was primarily restricted to capillaries, but tracer was still detected outside vessels (Fig. 1b, middle panel). In contrast, at E15.5, the tracer was confined to vessels with no detectable signal in the surrounding brain parenchyma, similar to the mature BBB (Fig. 1b, lower panel). The development of BBB functionality differed across brain regions (supplementary information, Extended Data Fig. 2). These data demonstrate that following vessel ingression into the neural tube, the BBB gradually becomes functional as early as E15.5.

Based upon the temporal profile of BBB formation, we compared expression profiles of BBB (cortex) and non-BBB (lung) endothelium at E13.5, using an Affymetrix array (supplementary information), and identified transcripts with significantly higher representation in cortical than lung endothelium (Fig. 2). These transcripts included transporters, transcription factors, and secreted and transmembrane proteins (Fig. 2c). We were especially interested in transmembrane proteins due to their potential involvement in cell-cell interactions that regulate BBB formation.

One of the genes identified, *Mfsd2a*, had 78.8 times higher expression in cortical endothelium compared to lung endothelium (Fig. 3a). *In situ* hybridization showed prominent *Mfsd2a* mRNA expression in CNS vasculature but no detectable signal in

vasculature outside the CNS, such as in lung or liver (Fig. 3b). Moreover, both *Mfsd2a* mRNA and MFSD2A protein were absent in the choroid plexus vasculature, which is part of the CNS but does not possess a BBB[1] (Fig. 3c,d and 3g). *Mfsd2a* expression in CNS vasculature was observed at embryonic stages (E15.5), postnatal days (P2 and P5) and in adults (P90) (Fig. 3b-e and Extended Data Fig. 4). Finally, MFSD2A protein which is absent in the *Mfsd2a*$^{-/-}$ mice (Fig. 3e)[21], was specifically expressed in Claudin-5-positive CNS endothelial cells but not in neighboring parenchyma cells (neurons/glia) or adjacent PDGFRβ-positive pericytes (Fig. 3f). Previously MFSD2A was reported to be a transmembrane protein expressed in the placenta and testis, which have highly restrictive barrier properties[22]. Together with our demonstration of *Mfsd2a* specific expression in BBB-containing endothelial cells, this suggests that *Mfsd2a* may play a role in BBB formation and/or function.

To test this hypothesis, we examined BBB integrity in *Mfsd2a*$^{-/-}$ mice. Using our embryonic injection method, 10-kDa dextran was injected into *Mfsd2a*$^{-/-}$ and wild-type littermates at E15.5. As expected, dextran was confined within vessels of control embryos. In contrast, dextran leaked outside the vessels in *Mfsd2a*$^{-/-}$ embryonic brains and was found in the cortical parenchyma (Fig. 4a) and individual parenchyma cells (quantified as tracer-positive parenchyma cells per unit area of the developing lateral cortical plate; Fig. 4b). Furthermore, using imaging and spectrophotometric quantification methods[5], we found that the leaky phenotype persisted in early postnatal (Extended Data Fig. 5) and adult (Fig. 4c) *Mfsd2a*$^{-/-}$ mice. Because the sequence of MFSD2A has similarities to the major facilitator superfamily of transporters, and MFSD2A facilitates the transport of tunicamycin in cancer cell lines[23], we injected two non-carbohydrate-based tracers of different sizes to rule out the possibility that dextran leakiness is due to interactions with MFSD2A. Sulfo-NHS-biotin (~550-Dalton) and horseradish peroxidase (HRP; ~44-kDa) tracers exhibited the leaky phenotype in *Mfsd2a*$^{-/-}$ mice (Extended Data Fig. 5a,b). Moreover, a larger molecular weight tracer, 70-kDa dextran, also displayed leakiness in *Mfsd2a*$^{-/-}$ mice (Extended Data Fig. 5d). In contrast to severe barrier leakage defects (Fig. 4a-c, Extended Data Fig. 5), brain vascular patterning between *Mfsd2a*$^{-/-}$ mice and littermate controls were similar. No abnormalities were identified in capillary density, capillary diameter or vascular branching (Fig. 4d, Extended Data Fig. 6a), in embryonic (E15.5), postnatal (P4), and adult (P70) brains of *Mfsd2a*$^{-/-}$ mice. Moreover, we found no abnormalities in cortical arterial distribution in adult *Mfsd2a*$^{-/-}$ mice (Extended Data Fig. 6b). Therefore, MSFD2A is specifically required for proper formation of a functional BBB but not for CNS vascular morphogenesis *in vivo*. This result, together with the temporal difference between cortical vascular ingression (E10-E11) and cortical barrier-genesis (E13.5-E15.5), demonstrates that vascular morphogenesis and barrier-genesis are distinct processes.

We next addressed if MFSD2A regulates endothelial tight junction formation, transcytosis, or both. We examined these properties by electron microscopy (EM) in embryonic brains and P90 mice following intravenous HRP injection[2]. EM failed to reveal any apparent abnormalities in the ultrastructure of endothelial tight junctions (Fig. 5a). At E17.5, tight junctions in control and *Mfsd2a*$^{-/-}$ littermates appeared normal, with electron-dense linear structures showing ‘kissing points’ where adjacent membranes are tightly apposed (Fig. 5a).

In electron micrographs of cerebral cortex in HRP-injected adults, peroxidase activity was revealed by an electron-dense reaction-product that filled the vessel lumen. In both control and *Mfsd2a*$^{-/-}$ mice, HRP penetrated the intercellular spaces between neighboring endothelial cells only for short distances. HRP was stopped at the tight junction, creating a boundary between HRP-positive and HRP-negative regions without leakage through tight junctions (Fig. 5a). In contrast, CNS endothelium of *Mfsd2a*$^{-/-}$ mice displayed a dramatic increase in the number of vesicles, including luminal and abluminal plasma membrane-connected vesicles and free cytoplasmic vesicles, which may indicate an increased rate of transcytosis (Fig. 5b). Specifically, pinocytotic events were evidenced by type II lumen-connected vesicles pinching from the luminal plasma membrane. Greater than 2-fold increases in vesicle number in *Mfsd2a*$^{-/-}$ mice compared to control littermates were observed in different locations along the transcytotic pathway (Fig. 5c, Extended Data Fig. 7a). Further, the HRP reaction product in adult mice was observed in vesicles invaginated from the luminal membrane and exocytosed at the abluminal plasma membrane only in *Mfsd2a*$^{-/-}$ mice (Fig. 5d), suggesting that HRP was subject to transcytosis in these animals but not in wild-type littermates (Extended Data Fig. 7b). Together, these findings suggest that the BBB leakiness observed in *Mfsd2a*$^{-/-}$ mice was not caused by opening of tight junctions, but rather by increased transcellular trafficking across the endothelial cytoplasm.

Studies using pericyte-deficient genetic mouse models have shown that pericytes can also regulate BBB integrity. These mice had increased vesicle trafficking without obvious junction defects[4, 5], similar to what we observed in *Mfsd2a*$^{-/-}$ mice. We therefore examined the possibilities that MFSD2A may regulate CNS endothelial transcytosis by modulating pericyte function or that the effect of pericytes on endothelial transcytosis is mediated by MFSD2A. First, pericyte coverage, attachment to the capillary wall, and pericyte ultrastructure and positioning relative to endothelial cells were normal in *Mfsd2a*$^{-/-}$ mice (Extended Data Fig. 8). These data, together with the lack of MFSD2A expression in pericytes, suggest that the increased transcytosis observed in *Mfsd2a*$^{-/-}$ endothelial cells is not secondary to pericyte abnormalities. Second, a genetic reduction in pericyte coverage can influence endothelial gene expression profiles[4, 5]. Therefore we analyzed published microarray data of two pericyte-deficient mouse models[5] and found a dramatic down-regulation of *Mfsd2a* in these mice, with a direct correlation between the reduction of *Mfsd2a* gene expression and the degree of pericyte coverage (Extended Data Fig. 9a). Further, immunostaining for MFSD2A in *Pdgfb*$^{ret/ret}$ mice[5] revealed a significant decrease in MFSD2A protein levels in endothelial cells that are not covered by pericytes (Extended Data Fig. 9b-d). Therefore, it is plausible that the increased vesicular trafficking phenotype observed in pericyte-deficient mice is, at least in part, mediated by MFSD2A, and that endothelial-pericyte interactions control the expression of MFSD2A which in turn controls BBB integrity.

We demonstrate that MFSD2A is required to suppress endothelial transcytotis in the CNS. Because of MFSD2A's involvement in human trophoblast cell fusion[24] and of our genetic evidence for its role in suppressing transcytosis, we hypothesize that MFSD2A serves as a cell surface molecule to regulate membrane fusion or trafficking. Indeed, from immuno-EM examination, MFSD2A protein was found in the luminal plasma membrane and associated

with vesicular structures in cerebral endothelial cells, but not in tight-junctions (Extended Data Fig. 10). At present, it is not clear whether the reported transporter function of MFSD2A is related to its role in BBB formation.

BBB breakdown has been reported in the etiology of various neurological disorders[7–10], and two separate *Mfsd2a* deficient mouse lines were reported to exhibit neurological abnormalities, such as ataxic behavior[21, 25]. Finding a novel physiological role of MFSD2A may provide a valuable tool to address how a non-functional BBB could affect brain development. In addition, our finding also highlights the importance of the transcytotic mechanism in BBB function, whereas most previous attention has been focused on potential BBB leaks through intercellular-junctions. Indeed, increased numbers of pinocytotic vesicles was observed following acute exposure to external stress inducers in animal models[26], and have also been observed in human pathological conditions[9]. It will be interesting to examine whether MFSD2A is involved in these pathological and acute assault situations. We cannot formally exclude but it is very unlikely that the elevated levels of transcytosis in *Mfsd2a*$^{-/-}$ mice was due to some form of acute cellular stress because under stress, cells either respond to return to homeostasis or cell death occurs[27]. However, increased transcytosis in *Mfsd2a*$^{-/-}$ mice persists from embryonic stages to adulthood, and up to six months old these mice exhibit no sign of vascular degeneration (Extended Data Fig. 6c). Our identification of a key molecular player in BBB formation may also aid efforts to develop therapeutic approaches for efficient drug delivery to the CNS. As an accessible cell surface molecule, MFSD2A is poised to be a potential therapeutic target for BBB restoration and manipulation.

## Methods summary

Wild-type Swiss-Webster mice (Taconic Farms, Inc.) were used for embryonic BBB functionality assays and expression profiles. Homozygous *Tie2-GFP* transgenic mice (Jackson laboratory, strain 003658) were used for BBB transcriptional profiling. *Mfsd2a* null mice[21] (MMRRC strain 032467-UCD) were maintained on C57Bl/6;129SVE mixed background and used for testing the involvement of MSFD2A in barrier-genesis. All animals were treated according to institutional and NIH guidelines approved by IACUC at Harvard Medical School.Deeply anaesthetized pregnant mice were used. Minimal volume of 10-kDa Dextran-Tetramethylrhodamine, Lysine Fixable (D3312 Invitrogen) was injected into the embryonic liver, while keeping the embryo connected to the maternal blood circulation through the umbilical cord. After three minutes of tracer circulation, embryonic heads were fixed by immersion in 4% paraformaldehyde (PFA) overnight at 4°C, cryopreserved in 30% sucrose and frozen in TissueTek OCT (Sakura). 12 μm sections were then collected and post fixed in 4% PFA at room temperature (RT) for 15 min, washed in PBS and co-stained with either α-PECAM antibody or with Isolectin B4 to visualize blood vessels (see Method section for details). P90 HRP injection and E17.5 cortex capillaries TEM imaging was done as previously described[2].

# Methods

## Animals

Wild-type Swiss-Webster mice (Taconic Farms, Inc.) were used for embryonic BBB functionality assays and expression profiles. Homozygous *Tie2-GFP* transgenic mice (Jackson laboratory, strain 003658) were used for BBB transcriptional profiling. *Mfsd2a* null mice[23] (Mouse Biology Program, University of California, Davis - MMRRC strain 032467-UCD, B6;129S5-Mfsd2atm1Lex/Mmucd) were maintained on C57Bl/6;129SVE mixed background and used for testing the involvement of MSFD2A in barrier-genesis. *Mfsd2a* null mutant mice were genotyped using the following PCR primers:

5’ CCTGGTTTGCTAAGTGCTAGC and 5’ GTTCACTGGCTTGGAGGATGC – which provide a 210 bp product for the *Mfsd2a* wild-type allele.

5’ CACTTCCTAAAGCCTTACTTC and 5’ GCAGCGCATCGCCTTCTATC – which provide a 301 bp product for the *Mfsd2a* knockout allele.

Pregnant mice were obtained following overnight mating (day of vaginal plug was defined as embryonic day 0.5).

All animals were treated according to institutional and NIH guidelines approved by IACUC at Harvard Medical School. Deeply anaesthetized pregnant mice were used.

## Immunohistochemistry

Tissues were fixed with 4% paraformaldehyde (PFA) at 4°C overnight, cryopreserved in 30% sucrose and frozen in TissueTek OCT (Sakura). Tissue sections were blocked with 5% goat serum, permeabilized with 0.5% Triton X-100, and stained with the following primary antibodies: α-PECAM (1:500; 553370, BD PharmingenTM), α-Claudin5 (1:400; 35-2500, Invitrogen), α-MFSD2A (1:500; Cell Signaling Technologies (under development)), α-PDGFRβ (1:100; 141402, eBioscience), α-CD31 (1:100; 558744, BD PharmingenTM), α-SMA (1:100, C6198, Sigma Aldrich), followed by 568/488 Alexa Fluor-conjugated secondary antibodies (1:300-1:1000, Invitrogen) or with Isolectin B4 (1:500; I21411, Molecular Probes). Slides were mounted in Fluoromount G (EMS) and visualized by epifluorescence, light, or confocal microscopy.

## *In situ* hybridization

Tissue samples were frozen in liquid nitrogen and embedded in TissueTek OCT (Sakura). Sections (18 μm) were hybridized with a digoxigenin (DIG)-labelled mouse *Mfsd2a* antisense riboprobe (1,524–2,024bp NM_029662) at 60°C overnight. A sense probe was used to ensure signal specificity. For detection, signals were developed using anti-DIG antibody conjugated with alkaline phosphatase (Roche). After antibody treatment, sections were incubated with BM Purple AP Substrate (Roche).

## Embryonic BBB permeability assay

The method is based on the well-established adult BBB dye injection assay with special considerations for the injection site and volume to cater the nature of embryonic vasculature[20, 28–30]. Four major modifications were made:

1. Embryos were injected while still attached via the umbilical cord to the mother's blood circulation, minimizing abrupt changes in blood flow.
2. Taking advantage of the sinusoidal/fenestrated and most permeable liver vasculature, dye was injected using a Hamilton syringe into the embryonic liver and was taken into the circulation in a matter of seconds.
3. Dye volume was adjusted to a minimum that still allows detection in all CNS capillaries after 3 minutes of circulation (high fluoresce intensity dye enables the use of small volumes and facilitates detection at the single capillary level – 10-kDa Dextran-Tetramethylrhodamine, lysine Fixable (4 mg/ml D3312 Invitrogen, 1 μl for E13.5, 2 μl for E14.5, 5 μl for E15.5).
4. Traditional perfusion fixation was omitted, again to prevent damage to capillaries. Instead, fixable dyes were used to allow reliable immobilization of the dye at the end of the circulation time (relatively small embryonic brain facilitates immersion fixation). Embryonic heads were fixed by immersion in 4% paraformaldehyde (PFA) overnight at 4°C, cryopreserved in 30% sucrose and frozen in TissueTek OCT (Sakura). 12 μm sections were then collected and post fixed in 4% PFA at room temperature (RT) for 15 min, washed in PBS and co-stained with either α-PECAM antibody or with Isolectin B4 to visualize blood vessels. All embryos from each litter were injected blindly prior to genotyping.

### Postnatal and adult BBB permeability assay

P2-P5 pups were deeply anaesthetized and three methods were used:

1. 10 μl of 10-kDa/70-kDa Dextran-Tetramethylrhodamine (4 mg/ml D3312 Invitrogen) was injected into the left ventricle with a Hamilton syringe. After 5 min of circulation, brains were dissected and fixed by immersion in 4% PFA at 4°C overnight, cryopreserved in 30% sucrose and frozen in TissueTek OCT (Sakura). 12 μm sections were collected and post fixed in 4% PFA at RT for 15 min, washed in PBS and co-stained to visualize blood vessels with either α-PECAM primary antibody (1:500; 553370, BD Pharmingen™), followed by 488-Alexa Fluor conjugated secondary antibody (1:1000, Invitrogen) or with Isolectin B4 (1:500; I21411, Molecular Probes).
2. 10 μl of HRP Type II (5 mg/ml P8250-50KU Sigma-Aldrich) were injected into the left heart ventricle with a Hamilton syringe. After 5 min of circulation brains were dissected and immersion fixed in 2% glutaraldehyde in 4% PFA in cacodylate buffer (0.1 M, pH 7.3) at RT for 1 hour then at 4°C for 3 hours then washed in cacodylate buffer overnight. 100 μm cortical vibratome sections were processed in a standard DAB reaction.
3. EZ-link sulfo NHS Biotin was used as a tracer as described before[17].

### Imaging

Nikon Eclipse 80i microscope equipped with a Nikon DS-2 digital camera was used to image HRP tracer experiments, vasculature density and pericyte coverage comparisons and

expression analyses. Zeiss LSM 510 META upright confocal microscope was used to image Dextran and NHS-Sulfo-biotin BBB permeability assays. Nikon FluoView™ FV1000 laser scanning confocal microscope and Leica SP8 laser scanning confocal microscope were used for imaging MFSD2A and pericyte marker immunohistochemistry. Images were processed using Adobe Photoshop and ImageJ (NIH).

### Morphometric analysis of vasculature

25 μm-thick coronal sections of E15.5, P4 and P70 brains were immunostained for PECAM. For vascular density and branching, confocal images were acquired with a Nikon FluoView™ FV1000 laser scanning confocal microscope and maximal projection images (5 per animal) were used for quantifications. The number of branching points was manually counted. Capillary density was quantified using MetaMorph software (Universal Imaging, Downingtown, PA) by measuring the area occupied by PECAM-positive vessels per cortical area. The mean capillary diameter was measured manually in ImageJ from cross-sectional vascular profiles (20 per animal) on micrographs (5–7 per animal) taken under a 60x objective with a 2x digital zoom.

For artery distribution quantification, 25 μm-thick sections (P60) were stained for smooth muscle actin (SMA) and PECAM. The proportion of PECAM-positive brain vessels with artery (SMA) identity was quantified using MetaMorph and expressed as percent of controls. Quantification was done blindly.

### Quantification of cortical vessel pericyte coverage

Pericyte coverage of cortex vessels in *Mfsd2a*$^{-/-}$ and wild-type littermates control mice was quantified by analyzing the proportion of total Claudin5-positive endothelial length also positive for the pericyte markers CD13- or PDGFR-β. Immunostaining was performed on 20μm sections of P5 cortex. In each animal 20 images of 10 different sections were analyzed.

Microvasculature was found to be completely covered by pericytes in both *control* and *Mfsd2a*$^{-/-}$ mice and therefore no error bars are presented for the average pericyte coverage in Fig. S9 a-b. (n = 3). All the Analysis was done with ImageJ (NIH). Quantification was done blindly.

### Quantification of vessel leakage

Epi-fluorescence images of sections from injected tracer and co-stained with lectin were manually analyzed with ImageJ (NIH). 12 μm coronal cortical sections of the same rostral-caudal position were used for the analysis. The same acquisition parameters were applied to all images and same threshold was used. Tracer positive cells found outside a vessel (parenchyma) were used as a parameter for leakage. For each embryo, at least 20 sections of a fixed lateral cortical plate area were scored. Four arbitrary leakage groups were classified based on the number of tracer parenchyma positive cells per section (0, 1–5, 5–10, and 10–40). Average representation of each leakage group was calculated for *Mfsd2a*$^{-/-}$ and control embryos. Quantification was done blindly.

Spectrophotometric quantification of 10-kDa fluoro-ruby-dextran tracer was done from cortical extracts, 16hr after tail vein injections in adult mice, as described before[5].

### Transmission electron microscopy

TEM imaging of P90 HRP injection and E17.5 cortex capillaries was done as previously described[2]. 10 mg (per 20 g) of horseradish peroxidase (Sigma Aldrich, HRP , type II) were dissolved in 0.4 ml of PBS and injected into the tail veins of deeply anaesthetized P90 mice. After 30 min of HRP circulation, brains were dissected and fixed by immersion in a 0.1M sodium cacodylate- buffered mixture (5% glutaraldehyde and 4% PFA) for 1 hr at room temperature (RT) followed by 5 hr in PFA at 4°C. Following fixation, the tissue was washed overnight in 0.1 M sodium cacodylate buffer and then cut in 50 μm-thick free floating sections using a vibrotome. Sections were incubated for 45 min at RT in 0.05 M Tris-HCl pH 7.6 buffer, containing 5.0 mg/10 ml of 3–3' diaminobenzidine (DAB, Sigma Aldrich) with 0.01% hydrogen peroxide. Sections were then post-fixed in 1% osmium tetroxide and 1.5 % potassium ferrocyanide and dehydrated and embedded in epoxy resin. E17.5 samples were processed as the P90 samples without HRP injection and with longer fixation times (2–3 days in room temperature). Ultrathin sections (80 nm) were then cut from the block surface, collected on copper grids, stained with Reynold's lead citrate and examined under a 1200EX electron microscope (JEOL) equipped with a 2k CCD digital camera (AMT).

### Immunogold labeling for EM

Mice were deeply anesthetized and perfused through the heart with 30ml of PBS followed by 150 ml of a fixative solution (0.5% glutaraldehyde in 4% PFA prepared in 0.1 mM phosphate buffer, PB, pH 7.4), and then by 100 ml of 4% PFA in PB. The brain was removed and post fixed in 4% PFA (30 min, 4°C) and washed in PBS. 50 μm-thick coronal brain sections were cut the same day with a vibratome and processed free-floating. Sections were immersed in 0.1% sodium borohydride in PBS (20 min, RT), rinsed in PBS, and preincubated (2 hr) in a blocking solution of PBS containing 10% normal goat serum, 0.5% gelatine and 0.01% Triton. Incubation (24 hr, RT) with rabbit anti-MFSD2A (1:100; Cell Signaling Technologies (under development)) primary antibody was followed by rinses in PBS and incubation (overnight, RT) in a dilution of gold-labeled goat anti-rabbit IgGs (1:50; 2004, Nanoprobes). After washes in PBS and sodium acetate, the size of immunogold particles was silver-enhanced and sections rinsed in PB before processing for electron microscopy.

### Statistical analysis

Comparison between wild-type and *Mfsd2a*$^{-/-}$ pericyte coverage and spectrophotometric quantification of 10-kDa fluoro-ruby-dextran tracer leakage was performed by a Mann–Whitney U test (appropriate for small sample size - each embryo was considered as a sample). An unpaired student's *t*-test was used (GraphPad Prism 4 Software) for comparison between wild-type and *Mfsd2a*$^{-/-}$ for vascular density, artery distribution, number of vesicular types, mean capillary diameter and MFSD2A expression in pericyte deficient mice. $P < 0.05$ was considered significant (StatXact (Cytel Software Corporation, Cambridge, MA, USA).

### Transcriptional profiling

E13.5 *Tie2-GFP* embryos were micro-dissected for cortex and lungs. Cortex tissue was carefully cleared of the meninges and choroid plexus. FACS purification of GFP positive cells and GeneChip analysis was performed as previously described[31]. RNA was purified with Arcturus PicoPure RNA isolation kit (Applied biosystems™), followed by NuGEN Ovation V2 standard linear amplification and hybridization to Affymetrix Mouse Genome 430 2.0 Array. All material from a single litter (10–13 embryos) was pooled and considered as a biological replicate. Four biological replicates were used. Each biological replicate represents purification from different litters performed on different days.

### Transcriptional profile analysis of pericyte deficient mice

Expression data from pericyte deficient mice generated by Armulik et al.[5] were obtained from the Gene Expression Omnibus (http://www.ncbi.nlm.nih.gov/geo, GSE15892). All microarrays were analyzed using MAS5 probe set condensation algorithm with Expression Console software (Affymetrix). P-value was determined using a two tailed student's *t*-test (n = 4).

### MFSD2A protein expression in *Pdgfb*$^{ret/ret}$ mice

Brain samples from P10-P14 mice and controls were kindly provided by Dr. Christer Betsholtz. Samples processing and immunohistochemistry was done as described for all other samples in our study. MFSD2A staining quantification was done with 12 μm cortical sagital sections. Confocal images were acquired with Nikon FluoView™ FV1000 laser scanning confocal microscope. Quantification of mean gray value per vascular profile was done with ImageJ (NIH) by outlining vascular profiles according to lectin staining and measuring MFSD2A intensity in these areas. In all images, PDGFRβ antibody staining was used to test presence of pericytes in quantified vessels. n = 2 animals per genotype, 60 images quantified of at least 600 vascular profiles per animal. Quantification was done blindly.

## Supplementary Material

Refer to Web version on PubMed Central for supplementary material.

## Acknowledgments

We thank Drs. Morris Karnovsky, Elio Raviola and Thomas Reese for guidance; Drs. Bob Datta, Charles Weitz, Michael Greenberg, Qiufu Ma, Chris Harvey and members of the Gu laboratory for comments on the manuscript; Drs. David Sabatini and Jan Reeling for sharing unpublished data; Dr. Christer Betsholtz and Cecilia Olsson for providing *Pdgfb*$^{ret/ret}$ mouse brain samples; Drs. Tom Schwarz and Asli Oztan for discussions and advice on cell trafficking; Dr. Won-Jong Oh for help with graphic illustrations; the Flow Cytometry Facility in the department of Systems Biology at Harvard Medical School for cell sorting, the Microarray Core at Dana-Farber Cancer Institute for Affymetrix assay; the Enhanced Neuroimaging Core at Harvard NeuroDiscovery Center for helping with confocal imaging and image analysis; the HMS Electron Microscopy Core Facility, the Neurobiology Imaging Facility for consultation and instrument availability that supported this work (This facility is supported in part by the Neural Imaging Center as part of an NINDS P30 Core Center grant #NS072030); Drs. Roberto Polakiewicz and Jianxin Xie from CST for generating MFSD2A antibodies. This work was supported by the Harold Perlman postdoctoral fellowships (A.B.Z.), the Goldenson postdoctoral fellowship (A.B.Z), the Lefler postdoctoral fellowship (A.B.Z), the DFG-German Research Foundation postdoctoral fellowship (E.K.), the Mahoney postdoctoral fellowship (B.L.), NIH training grant 5T32MH20017-15 (B.J.A), and the following grants to C.G.:

Sloan research fellowship, Armenise junior faculty award, the Genise Goldenson fund, the Freudenberger award, and NIH grant R01NS064583.

## References


1. Saunders NR, Liddelow SA, Dziegielewska KM. Barrier mechanisms in the developing brain. Front Pharmacol. 2012; 3:46. [PubMed: 22479246]
2. Reese TS, Karnovsky MJ. Fine structural localization of a blood-brain barrier to exogenous peroxidase. J Cell Biol. 1967; 34:207–217. [PubMed: 6033532]
3. Siegenthaler JA, Sohet F, Daneman R. 'Sealing off the CNS': cellular and molecular regulation of blood-brain barriergenesis. Curr Opin Neurobiol. 2013; 13:001256.
4. Daneman R, Zhou L, Kebede AA, Barres BA. Pericytes are required for blood– brain barrier integrity during embryogenesis. Nature. 2010; 468:562–566. [PubMed: 20944625]
5. Armulik A, et al. Pericytes regulate the blood–brain barrier. Nature. 2010; 468:557–561. [PubMed: 20944627]
6. Bell RD, et al. Pericytes Control Key Neurovascular Functions and Neuronal Phenotype in the Adult Brain and during Brain Aging. Neuron. 2010; 68:321–323. [PubMed: 21040834]
7. Zlokovic BV. The blood-brain barrier in health and chronic neurodegenerative disorders. Neuron. 2008; 57:178–201. [PubMed: 18215617]
8. Zhong Z, et al. ALS-causing SOD1 mutants generate vascular changes prior to motor neuron degeneration. Nature Neuroscience. 2008; 11:420–422.
9. Bell RD, Zlokovic BV. Neurovascular mechanisms and blood-brain barrier disorder in Alzheimer's disease. Acta Neuropathol. 2009; 118:103–113. [PubMed: 19319544]
10. Bell RD, et al. Apolipoprotein E controls cerebrovascular integrity via cyclophilin A. Nature. 2012; 485:512–516. [PubMed: 22622580]
11. Saunders NR, et al. Transporters of the blood–brain and blood–CSF interfaces in development and in the adult. Mol Aspects Med. 2013; 34:742–752. [PubMed: 23506907]
12. Stenman JM, et al. Canonical Wnt signaling regulates organ-specific assembly and differentiation of CNS vasculature. Science. 2008; 322:1247–1250. [PubMed: 19023080]
13. Liebner S, et al. Wnt/beta-catenin signaling controls development of the blood-brain barrier. J. Cell Biol. 2008; 183:409–417. [PubMed: 18955553]
14. Daneman R, et al. Wnt/b-catenin signaling is required for CNS but not non-CNS, angiogenesis. Proc. Natl Acad. Sci. USA. 2009; 106:641–646. [PubMed: 19129494]
15. Tam SJ, et al. Death receptors DR6 and TROY regulate brain vascular development. Dev Cell. 2012; 22:403–417. [PubMed: 22340501]
16. Cullen M, et al. GPR124, an orphan G protein-coupled receptor, is required for CNSspecific vascularization and establishment of the blood-brain barrier. Proc Natl Acad Sci U S A. 2011; 108:5759–5756. [PubMed: 21421844]
17. Wang Y, et al. Norrin/Frizzled4 Signaling in retinal vascular development and blood brain barrier plasticity. Cell. 2012; 151:1332–1344. [PubMed: 23217714]
18. Alvarez JI, et al. The Hedgehog pathway promotes blood-brain barrier integrity and CNS immune quiescence. Science. 2011; 334:1727–1731. [PubMed: 22144466]
19. Mizee MR, et al. Retinoic acid induces blood–brain barrier development. J. Neurosci. 2013; 33:1660–1671. [PubMed: 23345238]
20. Stern L, Rapoport JL, Lokschina ES. Le fonctionnement de la barrière hématoencéphalique chez les nouveau-nés. C. R. Soc. Biol. 1929; 100:231–223.
21. Tang T, et al. A mouse knockout library for secreted and transmembrane proteins. Nat Biotechnol. 2010; 28:749–755. [PubMed: 20562862]
22. Esnault CA. placenta-specific receptor for the fusogenic, endogenous retrovirusderived, human syncytin-2. Proc Natl Acad Sci USA. 2008; 105:17532–72008. [PubMed: 18988732]
23. Reiling JH, et al. A Haploid genetic screen identifies the major facilitator domain containing2A (MFSD2A) transporter as a key mediator in the response to tunicamycin. Proc Natl Acad Sci U S A. 2011; 108:11756–11765. [PubMed: 21677192]

24. Toufaily C, et al. MFSD2a, the Syncytin-2 receptor, is important for trophoblast fusion. Placenta. 2013; 34:85–88. [PubMed: 23177091]

25. Berger JH, Charron MJ, Silver DL. Major facilitator superfamily domaincontaining protein 2a (MFSD2A) has roles in body growth, motor function, and lipid metabolism. PLoS One. 2012; 7:e50629. [PubMed: 23209793]

26. Nag, S. Pathophysiology of the blood-brain barrier breakdown. In: Nag, S., editor. The blood-brain barrier – biology and research protocols. Vol. 2. 2003. p. 99-100.Part

27. Chen F, Evans A, Pham J, Plosky B. Special review issue: Cellular stress responses. Molecular Cell. 2010; 40:2.

28. Ek CJ, Habgood MD, Dziegielewska KM, Saunders NR. Functional effectiveness of the blood-brain barrier to small water-soluble molecules in developing and adult opossum (Monodelphisdomestica). J. Comp. Neurol. 2006; 496:13–26. [PubMed: 16528724]

29. Risau W, Hallmann R, Albrecht U. Differentiation-dependent expression of proteins in brain endothelium during development of the blood-brain barrier. Dev Biol. 1986; 117:537–545. [PubMed: 2875908]

30. Bauer H, et al. Ontogenic expression of the erythroid-type glucose transporter (Glut 1) in the telencephalon of the mouse: correlation to the tightening of the blood-brain barrier. Brain Res Dev Brain Res. 1995; 26:317–325.

31. Daneman R, et al. The mouse blood-brain barrier transcriptome: a new resource for understanding the development and function of brain endothelial cells. PLoS One. 2010; 5:e13741. [PubMed: 21060791]

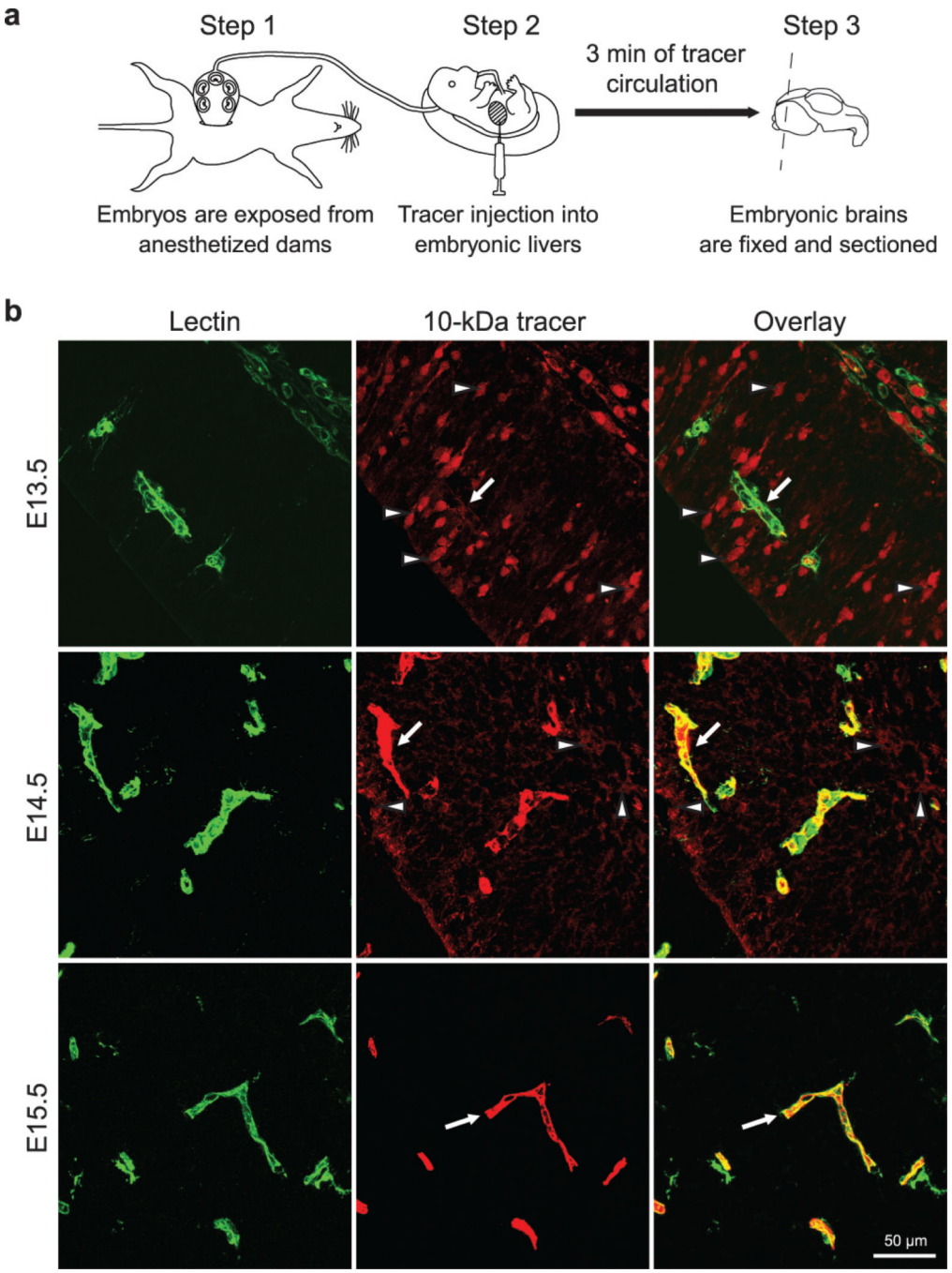


**Figure 1. A novel tracer injection method reveals a temporal profile of functional BBB formation in the embryonic cortex**

**a**, In-utero embryonic liver tracer injection method - fenestrated liver vasculature allowed rapid tracer uptake into the embryonic circulation. **b**, 10-kDa dextran-tracer injection revealed a temporal profile of functional cortical BBB formation. Representative images of dorsal cortical plates from injected embryos after capillary labeling with lectin (Green: lectin, red: 10-kDa tracer). Upper panel, E13.5: Tracer leaked out of capillaries and was subsequently taken up by non-vascular parenchyma cells (arrowheads), with little tracer left

inside capillaries (arrow). Middle panel, E14.5: Tracer was primarily restricted to capillaries (arrow), with diffused tracer detectable in the parenchyma (arrowheads). Lower panel, E15.5: Tracer was confined to capillaries (arrow). n=6 embryos (3 litters/age).

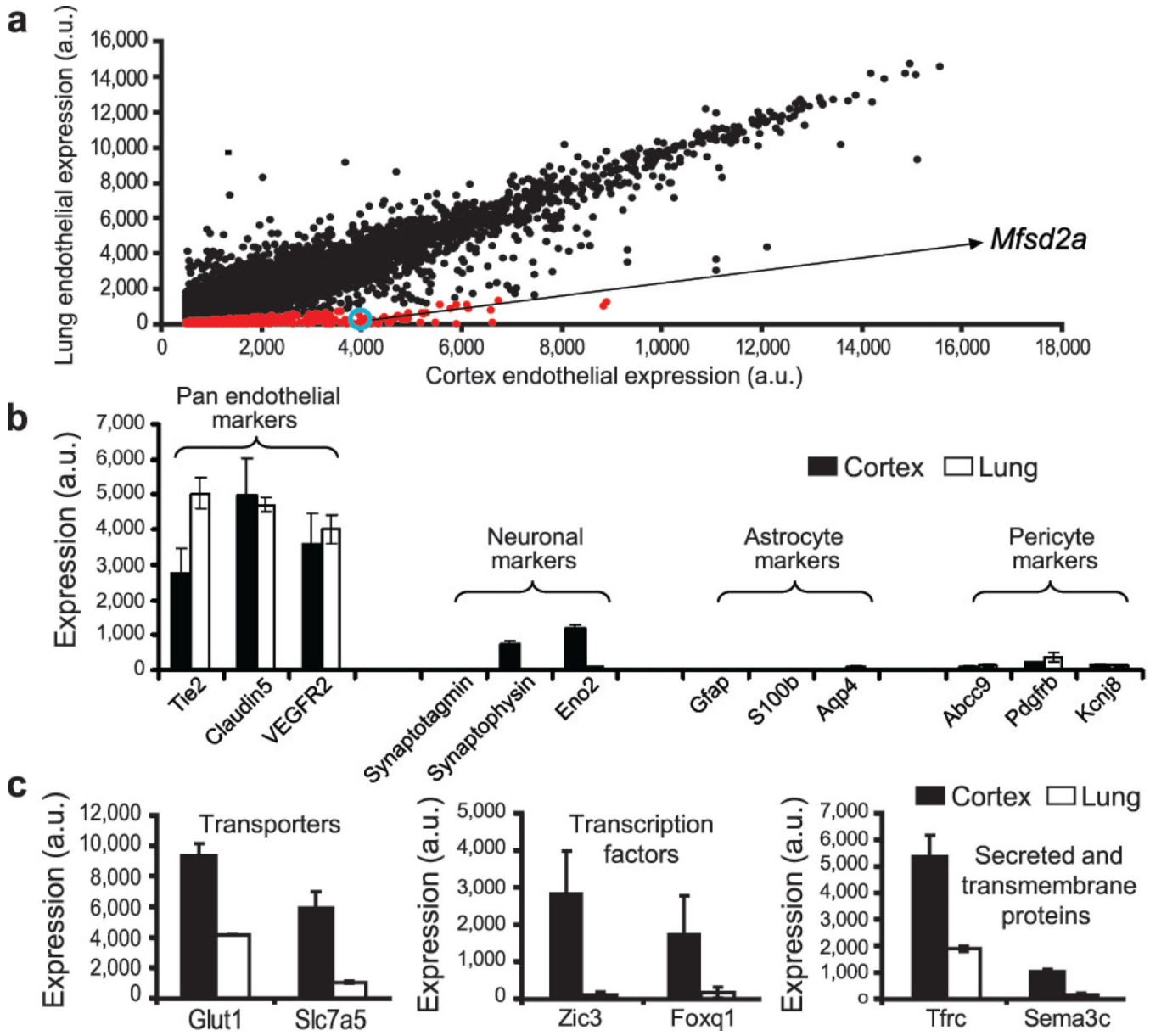


**Figure 2. Expression profiling identifies genes involved in BBB formation**

**a**, Dot plot representation of Affymetrix GeneChip data showing transcriptional profile of cortical (BBB) and lung (non-BBB) endothelial cells isolated at the critical barrier-genesis period (E13.5). Dots reflect average expression of a probe in the cortex (x-axis) and lung (y-axis). Cortex expression values above 500 arbitrary expression units (a.u) are presented. Red dots indicate a 5-fold higher expression in the cortex. *Mfsd2a* value is circled in blue. **b**, Pan-endothelial markers were highly represented, whereas pericyte, astrocyte, and neuronal markers were detected at extremely low levels in both cortex and lung samples. **c**, Barrier-genesis specific transporters, transcription factors, and secreted and transmembrane proteins were significantly enriched in the cortical endothelial cells. All data are mean±s.d. n=4 litters (4 biological replicates).

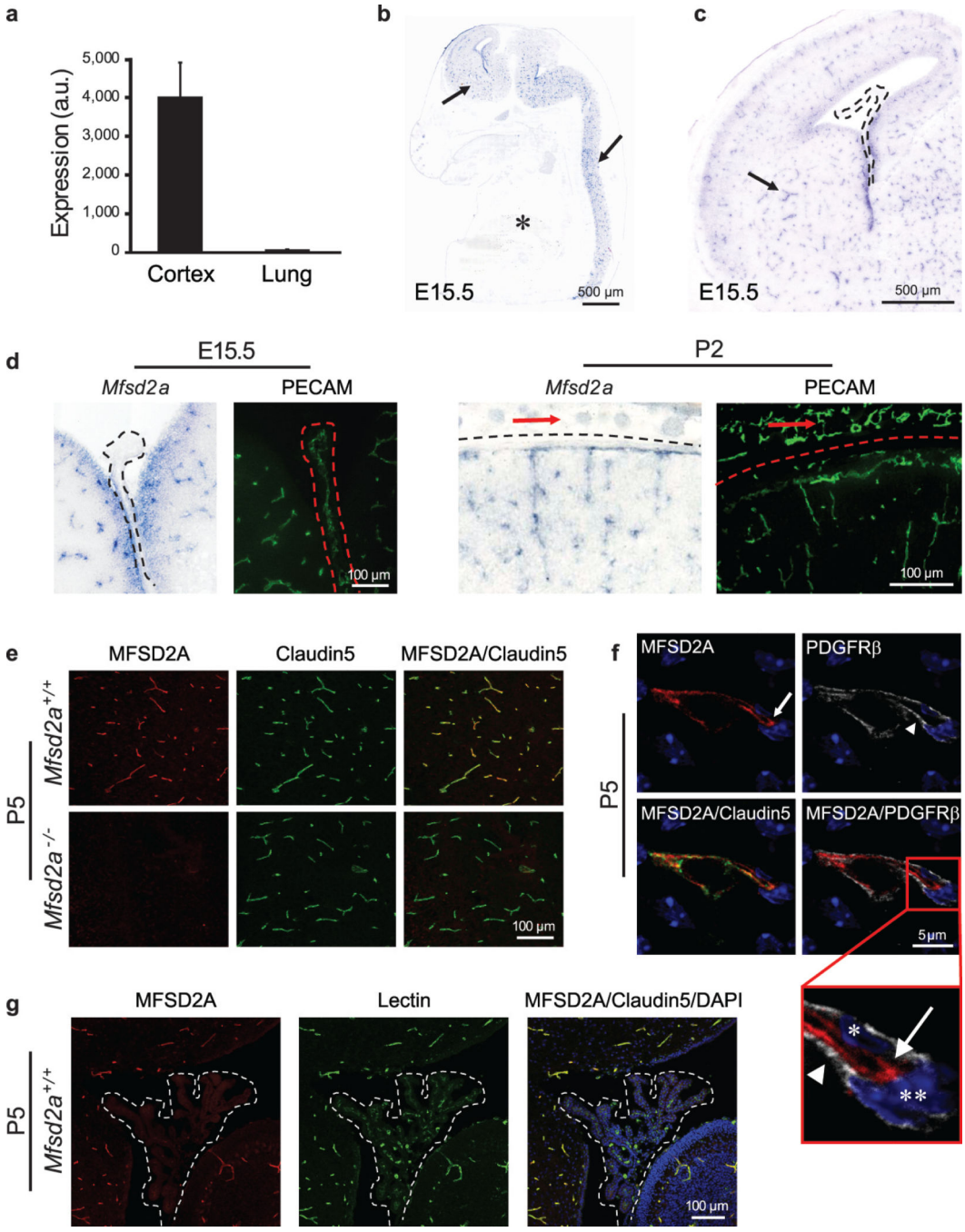


**Figure 3. *Mfsd2a* is selectively expressed in BBB-containing CNS vasculature**

**a**, E13.5: *Mfsd2a* expression in cortical endothelium was ~80-fold higher than lung endothelium (microarray analysis, mean±s.d.). **b-d**, Specific *Mfsd2a* expression in BBB-containing CNS vasculature (Blue: *Mfsd2a in situ* hybridization, green: vessel staining (PECAM) adjacent sections). **b**, *Mfsd2a* expression in CNS vasculature (E15.5 sagittal view-brain and spinal cord, arrows), but not in non-CNS vasculature (asterisk). **c**, *Mfsd2a* expression in BBB vasculature (E15.5 cortex coronal view, e.g. striatum, arrow), but not in non-BBB CNS vasculature (choroid plexus, dotted line). **d**, High magnification coronal

view of *Mfsd2a* expression in BBB-containing CNS vasculature but not in vasculature of the choroid plexus (left, dotted line), or outer meninges/skin (right, red arrows). **e-g**, Immunohistochemical staining of MFSD2A protein shows specific expression in CNS endothelial cells (Red: MFSD2A; green: Claudin5 or Lectin (endothelium); blue: DAPI (nuclei); gray: PDGFRβ (pericytes)). **e**, MFSD2A expression in the brain vasculature of wild-type mice (upper panel), but not of *Mfsd2a*$^{-/-}$ mice (lower panel). **f**, MFSD2A expression only in Claudin5-positive endothelial cells (arrow, endothelial nucleus–asterisk) but not in adjacent pericytes (arrow head, pericyte nucleus–double asterisk). **g**, Lack of MFSD2A expression in choroid plexus vasculature (fourth ventricle coronal view-dotted line), as opposed to the prominent MFSD2A expression in cerebellar vasculature. n=3 embryos (3 litters/age).

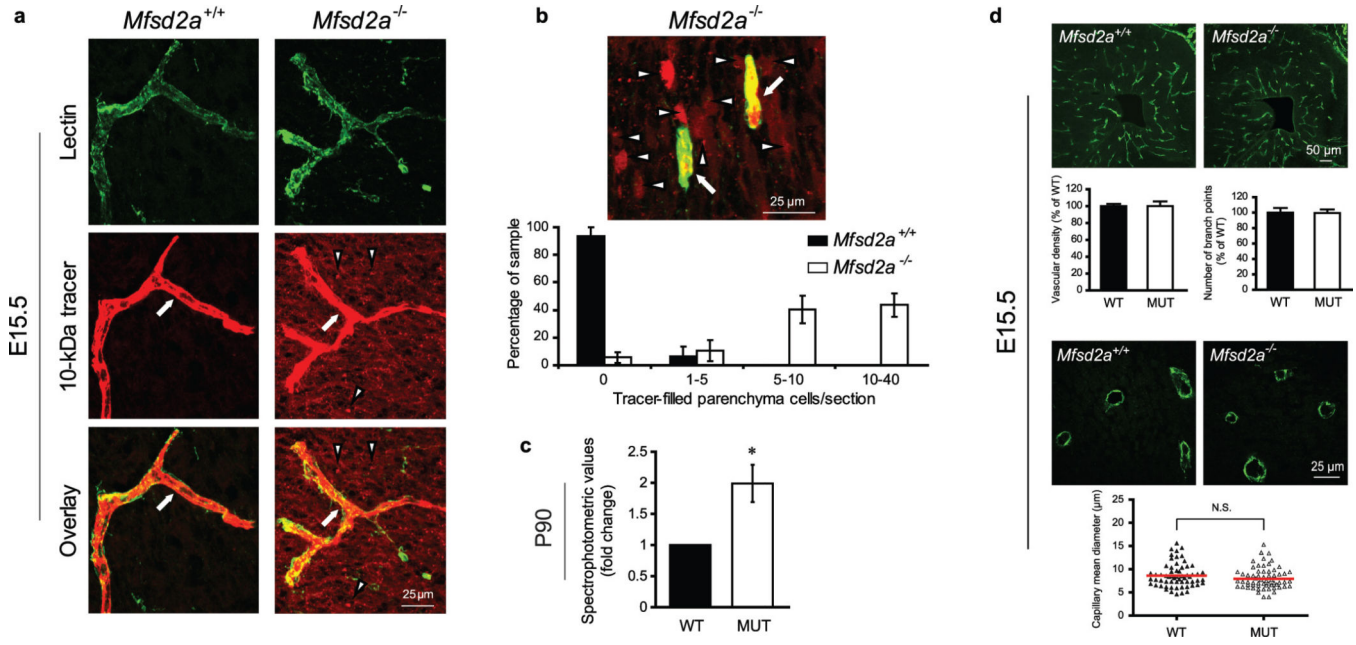


**Figure 4. *Mfsd2a* is required for the establishment of a functional BBB but not for CNS vascular patterning *in vivo***

**a,b**, 10-kDa dextran-tracer injections at E15.5 revealed a defective BBB in mice lacking *Mfsd2a*. **a**, The tracer was confined to the capillaries (arrow) in wild-type littermates, whereas *Mfsd2a*$^{-/-}$ embryos showed large amounts of tracer leakage in the brain parenchyma (arrowheads). **b**, Capillaries (arrows) surrounded by tracer-filled brain parenchyma cells (arrowheads) in *Mfsd2a*$^{-/-}$ cortex. Quantification of tracer-filled parenchyma cells in control versus *Mfsd2a*$^{-/-}$ cortical plates (lower panel n=7 embryos/genotype). **c**, Spectrophotometric quantification of 10-kDa dextran-tracer from cortical extracts, 16hr post i.v. injection, indicating that BBB leakiness in *Mfsd2a*$^{-/-}$ mice persists into adulthood (n=3 mice/genotype). **d**, *Mfsd2a*$^{-/-}$ mice exhibit normal vascular patterning. No abnormalities were found in cortical vascular density, branching and capillary diameter (E15.5, green: PECAM). Quantification of wild-type and *Mfsd2a*$^{-/-}$ samples (n=4 embryos/per genotype, (P>0.5)). All data are mean±s.e.m.

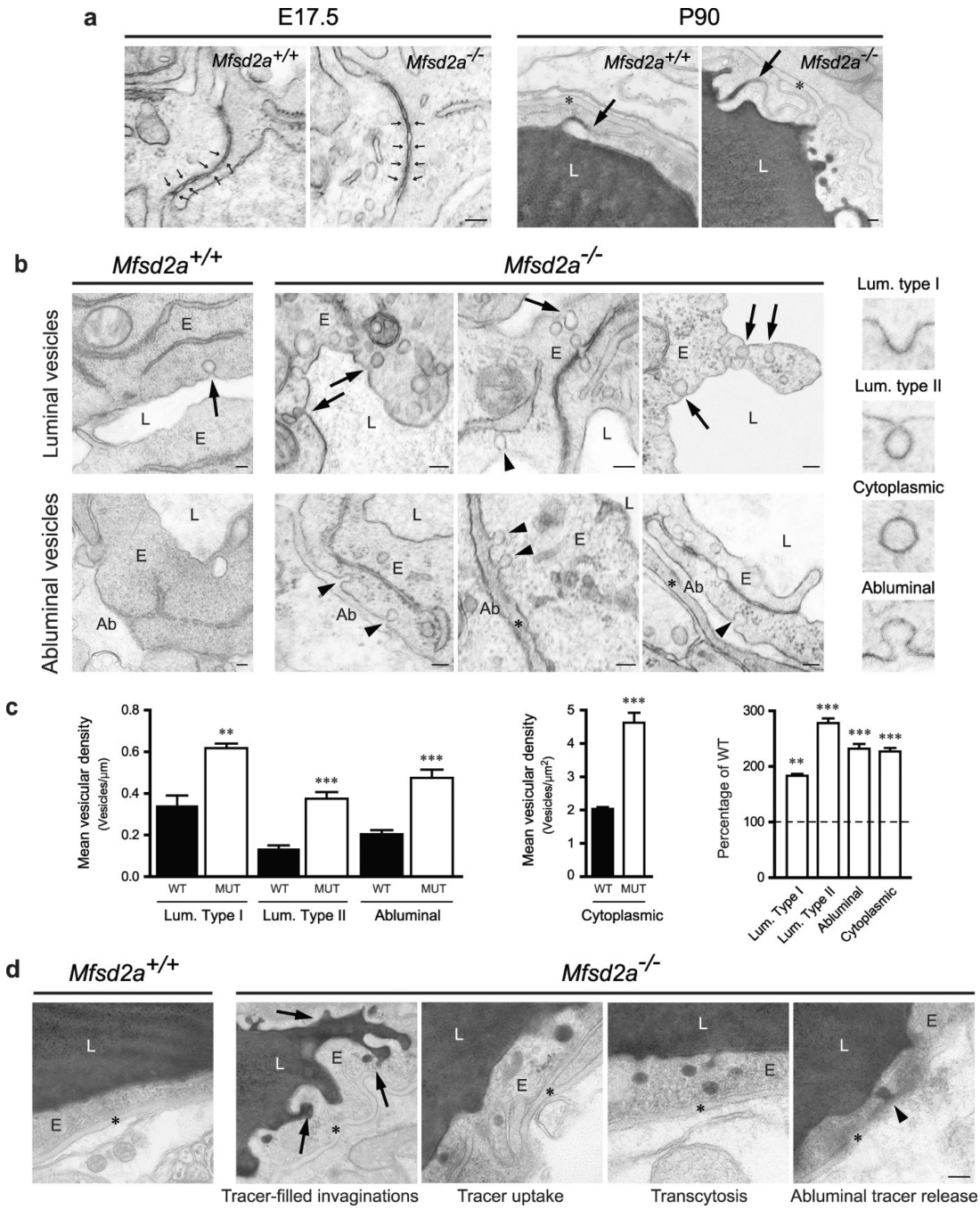


**Figure 5. *Mfsd2a* is required specifically to suppress transcytosis in brain endothelium to maintain BBB integrity**

Electron-microscopic examination of BBB integrity. **a**, Embryonic *Mfsd2a*$^{-/-}$ endothelium showed no overt tight-junction ultrastructural defect (normal "kissing points", small arrows, left). Vessel lumen in HRP-injected adult mice was filled with electron-dense DAB reaction (black) that diffused into intercellular clefts but stopped sharply at the junction without parenchymal leakage (arrows, right). **b**, Increased vesicular activity in embryonic *Mfsd2a*$^{-/-}$ endothelium (E17.5). **Left**, wild-type endothelium displayed very few vesicles (arrow).

**Right**, *Mfsd2a*$^{-/-}$ endothelium contained many vesicles of various types: luminal-(arrows), abluminal-(arrowheads) membrane-connected and cytoplasmic vesicles. **c**, Vesicular density quantification (as illustrated in b, see also Fig.S7a). **d**, Increased transcytosis was evident in HRP-injected adult *Mfsd2a*$^{-/-}$ mice (P90). In wildtype littermates (left) HRP activity was confined to the lumen with no HRP-filled vesicles. Many HRP-filled vesicles found in *Mfsd2a*$^{-/-}$ endothelial cells (right, see quantification Fig.S7b). Luminal invaginations (dye uptake, arrows) and release to the basement membrane (abluminal side (*)). Ab: abluminal, E: endothelium, L: lumen. Scale bars: a,b: 100 nm; c, 200 nm. All data are mean±s.e.m.